Chin. Geogra. Sci. 2022 Vol. 32 No. 4 pp. 580−591
https://doi.org/10.1007/s11769-022-1287-z

Springer Science Press
www.springerlink.com/content/1002-0063

Sandy Land-lake-vegetation Landscape of Songnen Sandy Land of China: Pattern, Process and Mechanism

DU Huishi[1], HASI Eerdun[2]

(1. *College of Tourism and Geographical Science*, *Jilin Normal University*, *Siping* 136000, *China*; 2. *Faculty of Geographical Science*, *Beijing Normal University*, *Beijing* 100875, *China*)

Abstract: In order to investigate the dynamic evolution of the sandy land-lake-vegetation landscape in Songnen Sandy Land (SSL) and its response to climate change and human activities, the distribution pattern, evolution, and driving mechanisms of the landscape were analyzed based on Landsat satellite images and meteorological and socio-economic data during 1980–2020. The results indicate that the area of sandy land exhibited an upward fluctuation during the last 40 yr, with a net increase of 251.75 km^2 at an increment rate of 3.80%/10 yr. The lake area also exhibited an upward fluctuation, with a net increase of 1200.95 km^2 at an increment rate of 20.42%/10 yr. Vegetation coverage decreased by 2633.30 km^2, with areas of low vegetation coverage exhibiting a trend of initial decline and subsequent increase, areas of medium vegetation coverage showed an upward fluctuation, and areas of high vegetation coverage showed a trend of initial increase and subsequent decrease, with overall changes of –0.67%/yr, 1.12%/yr, and 0.17%/yr, respectively. The relationships between sandy land, lakes, and vegetation coverage were significant, with areas of sandy land and low vegetation coverage showing the strongest correlation. The dynamic evolution of landscape is controlled by regional climatic and socio-economic factors, with socio-economic factors as the first principal component contributing up to 59.64%.

Keywords: sandy land; lake wetland; vegetation cover; landscape evolution; Songnen Sandy Land (SSL)

Citation: DU Huishi, HASI Eerdun, 2022. Sandy Land-lake-vegetation Landscape of Songnen Sandy Land of China: Pattern, Process and Mechanism. *Chinese Geographical Science*, 32(4): 580−591. https://doi.org/10.1007/s11769-022-1287-z

1 Introduction

Sandy land, lakes, and vegetation are sensitive to climatic fluctuations and human activities, and provide important information on global climate change and regional responses (Hulme and Kelly, 1993; Al-Masrahy and Mountney, 2015; Smith et al., 2021). The relationships between sandy lands, lakes, and vegetation in arid and semi-arid areas have been attracting the attention of scholars (Ackerly et al., 2015; Dong et al., 2016; An et al., 2021). To understand the coupling relationship between wind-sand activities and vegetation conditions, three scientific hypotheses have been put forward, based on which relevant research have been conducted (Abd El-Wahab et al., 2018). First, in arid and semi-arid sand areas, vegetation alters and controls near-surface wind-sand activities by changing wind momentum and wind speed, as well as partially retaining sand particles in near-surface airflow. Second, wind-sand flow affects vegetation colonization through erosion or burial (Mayaud et al., 2017). Third, lakes in sandy lands control wind-sand flow and vegetation by maintaining eco-

Received date: 2021-06-10; accepted date: 2021-10-09
Foundation item: Under the auspices of National Natural Science Foundation of China (No. 41871022), Natural Science Foundation of Jilin Province (No. 20210101398JC)
Corresponding author: HASI Eerdun. E-mail: hasi@bnu.edu.cn

logical functions, such as balanced wind-water interaction and soil moisture (Lancaster and Baas, 1998; Ma et al., 2016). Vegetation coverage can change sand particle movement, wind erosion speed, and wind speed profile height (Zhao et al., 2020) to some extent. As vegetation coverage increases, surface roughness also increases (Qiu et al., 2015). Different levels of vegetation coverage have different effects of blocking winds and changing the wind speed and flow field (Yang et al., 2017), which further leads to spatial differences in the sediment transport rate and erosion accumulation pattern (Heywood, 1941). In terms of the interaction between lakes and sandy lands, lakes affect the evolution process of sandy land by changing regional hydrological conditions, biogeochemical processes, plant communities, and their ecological functions (Hu et al., 2021). However, thus far, scholars have primarily been paying attention to interactions between only two of the three factors, and all three have rarely been analyzed in a unified manner.

Regarding the driving forces of changes in sandy land-lake-vegetation landscapes, scholars have focused on the impact of climate change on regional landscapes (Boulanger et al., 2017) or the response of regional landscape changes to climate fluctuations. Additionally, climate warming and drying processes during the last 30 yr (Bishop-Taylor et al., 2018) have undoubtedly been affecting the evolution process of landscapes in semi-arid areas. In the northern China, vegetation in the farming-pastoral ecotone has undergone drastic changes in the past decades, and it has been proven to be influenced by both natural and anthropogenic factors (Chen et al., 2021). Moreover, in rapidly developing China, socio-economic factors and national policies also shape the evolution of regional landscapes (Amuti and Luo, 2014; Hengeveld et al., 2017). For example, in the 1990s, large-scale lake-building projects caused the fragmentation of lake landscapes. However, after 2000, the project of returning farmland to wetlands and connecting rivers and lakes changed the pattern and characteristics of wetlands with high intensity in the short term. At present, it is urgent to carry out quantitative research on the contribution rate of climate factors and socio-economic factors. Accordingly, the relationships between aeolian sand, lakes, and vegetation, and the natural geographic units of specific basins are being determined through long-term remote sensing monitoring, so as to reveal the competition and balance relationship between aeolian sand, lakes, and vegetation, and further understand the evolution process of surface landscapes and their response to climate change.

Songnen Sandy Land (SSL) is located in the central and western part of the Northeast China Plain. It is a typical farming-pastoral ecotone and the sandy land with the largest population density and economic activity intensity in China. The ecological environment of this area is fragile, and the evolution of the surface landscape evolution is sensitive to global climate change and regional human activities. Satellite image data of recent decades show that the sandy land, lakes, and vegetation cover in this area have significantly changed. Thus, it serves as an ideal target area for studying the mechanism of sandy lands, lakes, and vegetation. In SSL, the evolution of sandy land (Yang and Zhang, 2012), the interaction between sandy land and vegetation, and the landscape evolution of lakes (Du et al., 2018a) have been discussed, but their interrelationships have not been explored. The main aim of this study is to elucidate the interaction mechanism of sandy land, lakes and vegetation. Therefore, this study investigated the characteristics of the sandy land-lake-vegetation landscape of SSL and its temporal and spatial evolution as well as its driving mechanisms from 1980 to 2020 based on 3S technology and mathematical statistical methods. The findings of this study will provide a scientific basis for the reconstruction of the ecological environment and regional sustainable development of SSL.

2 Materials and Methods

2.1 Study area

As the boundary of SSL is not consistently defined in the literature (Du et al., 2018a; Wang and Du, 2018), research initiatives are usually based on the areas defined by administrative divisions. Consequently, it is difficult to conduct comparative research and comprehensive analyses using the same spatial and temporal scales. From the perspective of natural geography, the development of sandy land in this area is controlled by regional wind and hydrodynamic forces. Hence, it is more scientific to define the boundaries of SSL using the watershed segmentation method (Du et al., 2018b). Based on Landsat 8 Operational Land Imager (OLI) images and Advanced Spaceborne Thermal Emission and Reflec-

tion Radiometer Global Digital Elevation Model (ASTER GDEM) data and with reference to the third-order regional boundary of the Songliao River Basin (Songliao Water Resources Commission of the Ministry of Water Resources, http://slwr.gov.cn/), in this study, the natural geographical unit of SSL was set as 43°00′28″N–50°36′51″N, 119°19′33″E–129°12′24″E, and its area was determined to be 352 559.12 km^2 (Fig. 1); the area of the sandy land was determined to be 1907.54 km^2.

SSL is located in the midwest of Songnen Plain. The area has a semi-arid and semi-humid climate, with an annual average temperature of 3.3°C and an annual precipitation of 360–480 mm. Annual precipitation is variable and unevenly distributed throughout the year. The annual evaporation is 1600–1800 mm. The annual windy days are 20–36 d, of which spring windy days account for 60%–68%. The zonal soil is chernozem, while the non-zonal soil comprises aeolian sandy soil, meadow soil, marsh soil, and saline-alkaline soil. The zonal vegetation is Baikal Stipa (*Stipa baicalensis*) and Gerbera (*Filifolium sibiricum*); non-zonal vegetation is characterized by eucalyptus grasslands, where the arbor comprises drought-tolerant Ulmus Campestris (*Ulmus pumila*), Pull Down Elm (*Ulmus macrocarpa varnata*) and Yellow Elm (*Ulmus macrocarpa*) and the shrubs are mainly Wild Apricot (*Armeniaca sibirica*), with Little Yellow Willow (*Salix gordejevii*) and Leaf Bead (*Securinega suffruticosa*) present in some areas. The sand-covered area is mainly located in the midwest of the research site. It is distributed on the floodplain, first-order terrace, and alluvial fan of the Nenjiang River and its tributaries, the second Songhua River, the Taoer River, and the Huolin River. The tectonic sedimentary structure belongs to the Songliao sedimentation. SSL is dominated by fixed and semi-fixed sand dunes, which include sand ridges, beam-shaped sand dunes, shrub-covered sand dunes, and gently flanked sand dunes. It is roughly divided by the line of Anda-Da'an-Qian'an-Tongyu, where the sand dune runs NW-SE in the west and SW-NE in the east. Lakes are widely distributed in the area. Their development is related to tectonic movement, crustal subsidence, and river course changes. The administrative districts include partial city (county) areas of Hulunbeier City, Xing'an League, Qiqihar City, Daqing City, Suihua City, Harbin City, Baicheng City, Songyuan City, Changchun City, and Jilin City.

2.2 Data source

The remote sensing data comprised Landsat Multispec-

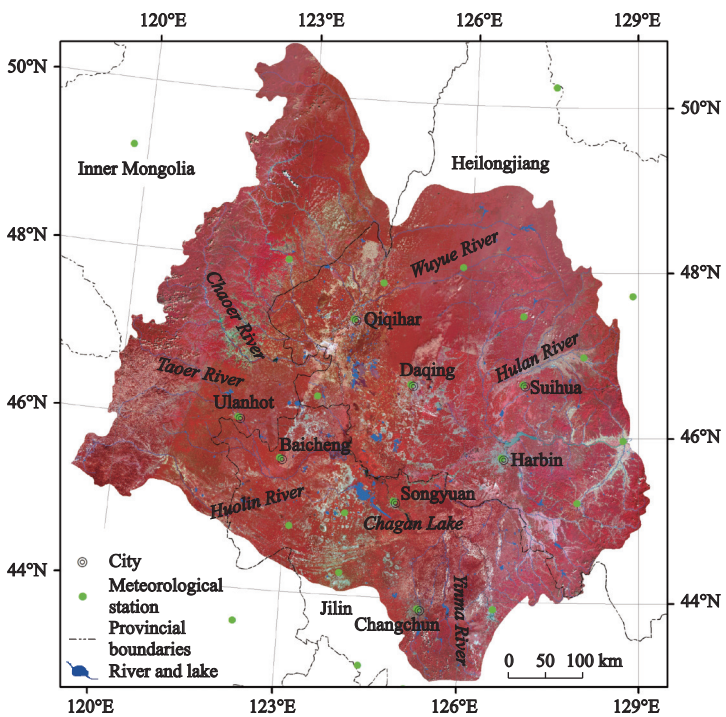

Fig. 1 Landsat OLI (Operational Land Imager) image of Songnen Sandy Land in 2020

tral Scanner (MSS), Thematic Mapper (TM), and OLI images for 1980, 1990, 2000, 2010, and 2020. The spatial resolutions of the MSS (1980), TM (1990, 2000, and 2010), and OLI (2020) images were 80 m, 30 m, and 30 m, respectively. All images were clear and acquired from mid-August to mid-September during the peak season of vegetation growth (US Geological Data Sharing Platform, http://glovis.usgs.gov/). The ERDAS 2010 software was used for image preprocessing, including band fusion, geometric fine correction (error control within one pixel), splicing, and cropping.

Regarding meteorological parameters, the annual average wind speed, annual precipitation, and annual average temperature from 17 meteorological stations in the research area during 1980–2020 were selected. These parameters have been considered by scholars as the main factors characterizing climate change (Wang et al., 2014; Wang et al., 2020). The 17 meteorological stations are Harbin, Tieli, Qiqihar, Shangzhi, Hailun, Tailai, Fuyu, Tonghe, and Keshan in Heilongjiang Province; Changchun, Fuyu, Baicheng, Qianan, Qian Gorlos, Tongyu, and Changling in Jilin Province; and Zhalantun in Inner Mongolia. The meteorological data were obtained from the China Meteorological Data Network (http://data.cma.cn/). The principle of the largest proportion of the area was adopted because the boundaries of the research site do not correspond fully to the boundaries of administrative divisions. Therefore, the socio-economic statistics of counties (cities, flags) with an area coverage greater than 70% of the total research site were used to analyze the influencing factors. Specific data used were local total population, gross domestic product (GDP), cultivated land area, and per capita GDP during 1980–2020. Scholars have reported that these indicators can suitably characterize socio-economic situations (Chen et al., 2020). The socio-economic data were obtained from the Statistical Yearbook (Statistical Bureau of Jilin Province, 2021; Statistical Bureau of Liaoning Province, 2021; Statistics Bureau of Inner Mongolia Autonomous Region, 2021).

2.3 Methodology

2.3.1 Object-oriented classification

Sandy land and lake information was extracted using the object-oriented method (Khatancharoen et al., 2021). To ensure complete utilization of the spectral information, geometric shape, texture features, and the relationship with other objects (Gutman and Ignatov, 1998), a scale of 200 was selected for multi-resolution segmentation of images at different stages. As most Landsat series images were mixed pixels, the shape of the area was relatively blurred. Compared with spectral features, shape features had less influence on image segmentation. Therefore, the weight parameters of shape heterogeneity h_{shape} and spectral heterogeneity h_{color} were set to 0.1 and 0.5, respectively. All bands were included in the extraction of sand information and given equal importance. Accordingly, the weight value of each band was set to 1. Based on the preliminary survey and using GPS for field verification points, eCognition 9.0 software was used to segment sandy land and lake information; the overall classification accuracy was 93% and the Kappa coefficient was 0.98.

2.3.2 Calculation of vegetation coverage

Within the scope of the study area, the interpretation range of sandy land and lake was removed using the mask method, and vegetation coverage over unclassified areas was calculated using the mixed pixel decomposition method; vegetation coverage information was retrieved from the vegetation index obtained from the original data after normalization (Carlson and Ripley, 1997):

$$F = ((NDVI - NDVI_{soil})/(NDVI_{veg} - NDVI_{soil}))^2 \quad (1)$$

where, F is the vegetation coverage, $NDVI_{soil}$ is the normalized difference vegetation index (NDVI) of bare or no vegetation coverage area, and $NDVI_{veg}$ is the $NDVI$ value of the pixel fully covered by vegetation pixel, the $NDVI$ value of the pure vegetation pixel (Steinberg et al., 2020).

For most bare fields, the $NDVI_{soil}$ value should theoretically be close to 0. When the vegetation reaches the state of full coverage, the $NDVI_{veg}$ value is close to 1. Considering the influence of different natural conditions such as time and geography, $NDVI$ is required to determine the $NDVI_{soil}$ and $NDVI_{veg}$ values of different images. By analyzing the $NDVI$ data of the Landsat series of images, combined with the actual situation of SSL and the cumulative probability distribution table of $NDVI$ values, the confidence level was determined to calculate vegetation cover at 0.5%. As farmlands are special vegetation areas, they should be removed during interpretation.

According to the classification standard of vegetation

coverage in the existing literature (Zhang and Li, 2018) and the site conditions of SSL, vegetation coverage in the study area was divided into three grades: low vegetation coverage ($F < 30\%$), medium vegetation coverage ($30\% \le F < 60\%$), and high vegetation coverage ($F \ge 60\%$).

2.3.3 Grey correlation degree

The grey system theory is used to comprehensively analyze the impact of climate change and socio-economic factors (Dong et al., 1996). The formula of the grey correlation degree is as follows:

$$r(X_0, X_i) = \frac{1}{n}\sum_{k=1}^{n} r(x_0(k), x_i(k)) \tag{2}$$

$$r(x_0(k), x_i(k)) = \frac{\min\limits_i \min\limits_k |x_0(k) - x_i(k)| + \rho \max\limits_i \max\limits_k |x_0(k) - x_i(k)|}{|x_0(k) - x_i(k)| + \rho \max\limits_i \max\limits_k |x_0(k) - x_i(k)|} \tag{3}$$

where r represents the grey correlation degree; $X_0 = \{x_0(1), x_0(2), \ldots, x_0(n)\}$ and $X_i = \{x_i(1), x_i(2), \ldots, x_i(n)\}$ are reference sequence (area) and comparison sequence (meteorological factors, socio-economic factors), respectively; n represents the total number of study periods; i represents the landscape category; k represents the time series; ρ represents the gray resolution coefficient, $\rho = 0.5$. In grey correlation degree analysis, the area of sandy land, the area of lakes, and the area of vegetation coverage all include 5 periods of data, and the total number of samples is 25. The software used in this research is Data Processing System (DPS) (v 9.50).

3 Results

3.1 Spatial pattern and evolution of sandy land-lake-vegetation landscape

3.1.1 Sandy land landscape

In SSL, sandy land is mainly distributed in the midwest (Fig. 2). In 1980, the sandy land was small and mainly distributed in the midwest and northeastern parts. In 1990, the area of the northeastern sandy land sharply decreased due to reclamation. Consequently, the center of sandy land shifted toward the southwest. In 2000, the sandy land area in the south continued to grow, with a relatively concentrated distribution. At that time, the area of sandy land reached its maximum of 2132.05 km^2. In 2010, the area of sandy land in the central part of the research site decreased. By 2020, the sandy land area in the south continued to decrease, which caused the cen-

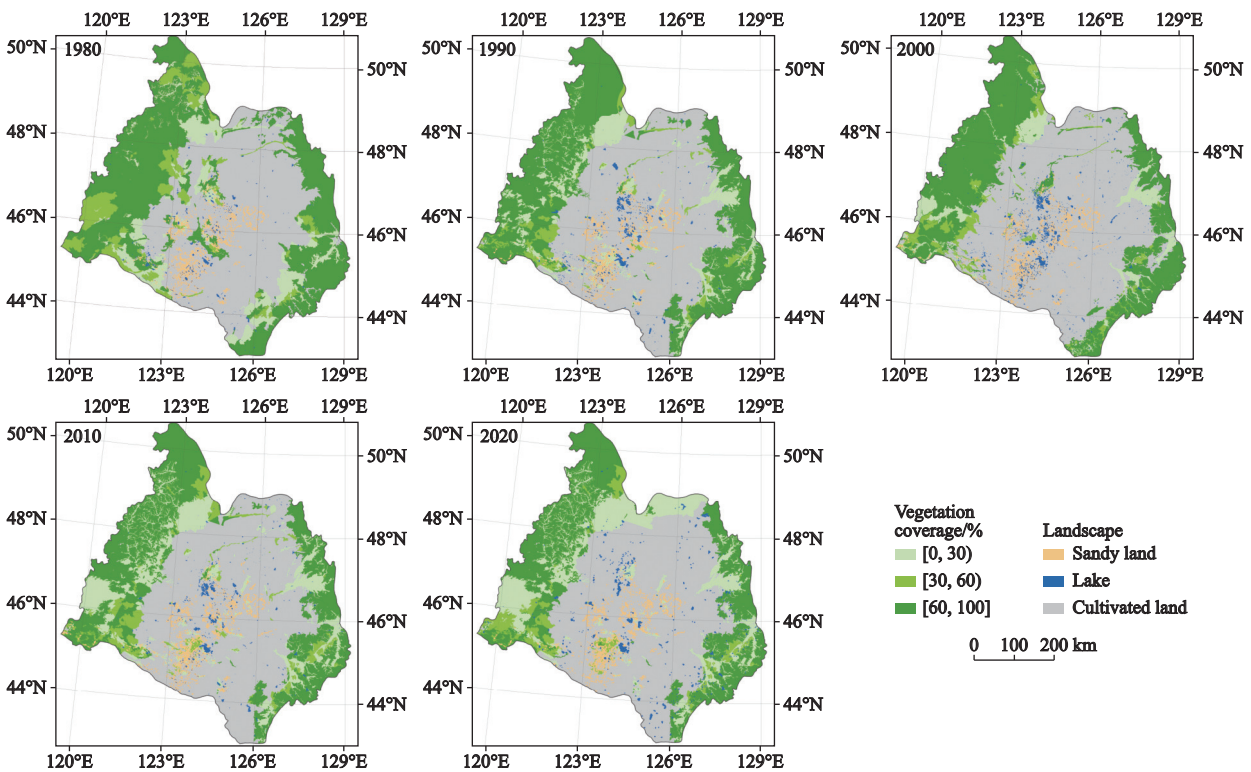

Fig. 2 Dynamic evolution of sandy land in SSL (Songnen Sandy Land)

ter of sandy land to migrate northeast. Overall, the sandy land area fluctuated upward during the last 40 yr. During 1980–2020, the area increased from 1655.79 km^2 to 1907.54 km^2, accounting for a change of 15.20%. Sandy land area increased continuously during 1980–2000, with a net growth of 475.26 km^2. During this period, the desertification phenomenon aggravated. While in 2000–2020, the sandy land area continued to shrink, accounting for a change of –5.97%, and the degree of desertification obviously declined.

3.1.2 Lake landscape

Lakes in SSL are mainly distributed in the Songyuan City and Daqing City (Fig. 2). During 1980–2020, the lake area fluctuated upward, with an overall change of 437.09 km^2 and an annual average increase of 0.80%. According to the characteristics of lake evolution, it can be divided into two periods with 2000 as the point of division. Lake evolution exhibited a trend of increase and decrease before and after 2000, respectively. The specific evolution process is as follows. During 1980–1990, the lake area increased from 1470.22 km^2 to 3493.64 km^2, an increase by 2023.42 km^2, which was mainly manifested by the increase of the water surface of large lakes such as Chagan Lake, Longhupao Lake and Aobaopao Lake. During 1990–2000, the lake area increased by 470.02 km^2, accounting for an increment of 13.44%, and reached the maximum of 3963.17 km^2 in 2000; after 2000, the lake area began to decrease, and shrank to 2671.17 km^2 in 2010, with an annual change of –3.3%. During 2010–2020, the lake area continued to decrease with an average annual change of –4.07%, which was mainly manifested by the sharp decrease in the water surface of lake wetlands in Daqing and Qiqihar, with typical areas such as Xihulupao Lake and Tiaohongpao Lake.

3.1.3 Vegetation landscape

Vegetation is mainly distributed in the west and east of the study area (Fig. 2). During the last 40 yr, the area of vegetation coverage showed a decreasing trend, with a net decrease of 2633.30 km^2. Areas with low and high vegetation cover decreased, while those with medium vegetation cover increased (Fig. 3). The area of low vegetation cover experienced a rapid decrease and then a slight increase. In general, the area of low vegetation cover decreased from 57 550.78 km^2 in 1980 to 42 053.95 km^2 in 2020, accounting for a change of –26.93%. The area of medium vegetation coverage displayed a pattern of increase-decrease-increase, and the area increased by 44.74% during last 40 yr. However, the area of high vegetation cover increased then subsequently decreased, and reached the maximum value of 112 317.64 km^2 in 2000, accounting for an overall change of 6.89%.

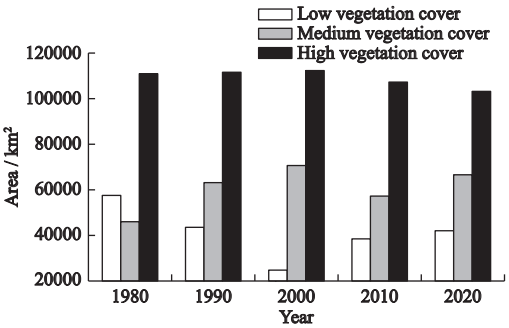

Fig. 3 Vegetation cover area change in SSL (Songnen Sandy Land)

3.1.4 Relationship between sandy lands, lakes, and vegetation

The sandy land area and areas of high, medium, and low vegetation coverage had a high degree of correlation at above 0.70 (Fig. 4). Moreover, it had a significant positive correlation with the area of medium vegetation coverage and a significant negative correlation with the area of low vegetation coverage(Fig. 4b). This is consistent with the findings of Dong et al. (1996). The degree of vegetation coverage determines the intensity of wind erosion. The rate of wind erosion in sandy land increases with decreasing vegetation coverage, which further decreases vegetation coverage and surface roughness. At a certain height above the sand surface, annual average wind speed gradually increases. As sand particles become less likely to get deposited, the wind erosion effect becomes more intense (Hesp and Smyth, 2017). Nevertheless, it is noteworthy that the coverage of natural and stable vegetation in sandy lands is generally less than 30%, and annual precipitation can infiltrate the deep soil or recharge groundwater, which is the basic eco-hydrological principle of the theory of sand control with low coverage (Yang et al., 2021).

The lake area was positively correlated with areas of high and medium vegetation coverage, but it had a significant negative correlation with the area of low vegetation coverage(Fig. 4c). There was a positive correlation between the sandy land and lake area. In the SSL, lakes are mainly distributed in sandy land, showing the characteristics of mosaic distribution and a dynamic

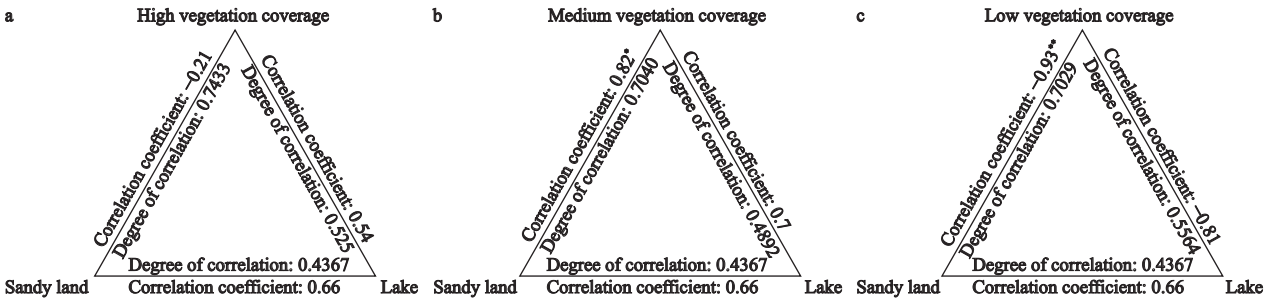

Fig. 4 Association between sandy land area, lake area, and areas of different vegetation coverage levels. * indicates significance at the 0.05 level, ** indicates significance at the 0.01 level

equilibrium relationship with trade-offs and interchanges.

3.2 Climate change and social and economic development

3.2.1 Climate change characteristics

During the study period covering past 40 yr, the annual average wind speed and annual precipitation showed downward fluctuations, while the annual average temperature showed an upward fluctuation. During 1980–1990, the annual average wind speed fluctuated minimally, and the annual average wind speed decreased at a rate of 0.20 (m·s)/10 yr (Fig. 5a). The annual precipitation as well as the annual average temperature fluctuated and increased. During this period, the lake water volume increased, resulting in the increase of the lake area. During 1990–2000, climate change was characterized by a continuous decrease in annual average wind speed, increase in annual precipitation(Fig. 5b), and upward fluctuation of annual average temperature(Fig. 5c). During this period, the volume of lake water continued to increase, and annual average temperature both increased, reducing the rate of increase in lake area. During 2000–2010, the annual average wind speed and annual precipitation both fluctuated downward, while the annual average temperature increased by 0.20°C/10 yr. The maximum annual precipitation was685.50 mm in 1998. From the perspective of a five-year moving average, the year of 2000 was the turning point of annual precipitation. Since then, the warming and drying trend of SSL has been obvious, resulting in the decrease of the volume of lake water and the shrinkage of lake area. During 2010–2020, the annual average wind speed and annual precipitation continued to decline, and the lake area continued to decrease.

3.2.2 Social and economic development

The total population, GDP, and cultivated land area increased, except for the large number of livestock at the end of the year (Fig. 6). The total population increased from 1980 to 2020, with a growth rate of 39.53% (Fig. 6a). With the rapid development of the regional economy, the GDP of SSL has increased exponentially (Fig. 6a), and the trend of change can be fitted by the exponential regression equation $y = 7E - 114e^{0.1343x}$ ($R^2 = 0.9936$). During the study period, the cultivated land area also showed an upward trend (Fig. 6b). It increased slowly during 1980–1999 and then increased sharply until 2000, after which it slowed down. The total cultivated land area increased by 12.48×10^4 km^2

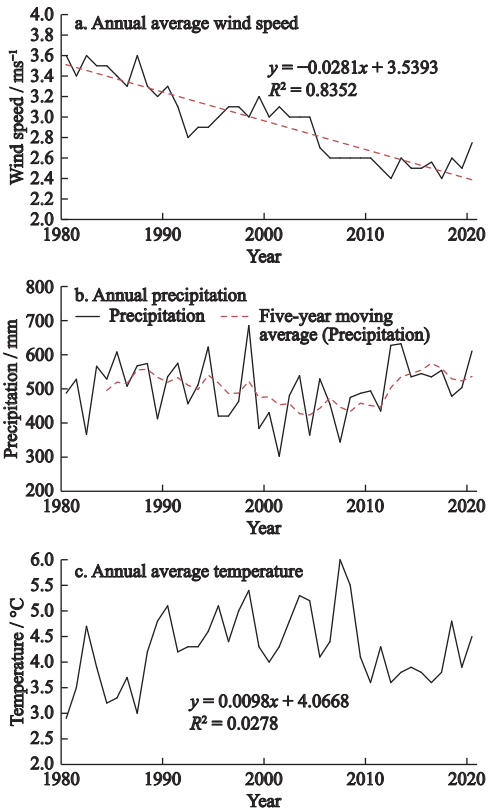

Fig. 5 Annual average meteorological data during 1980–2020

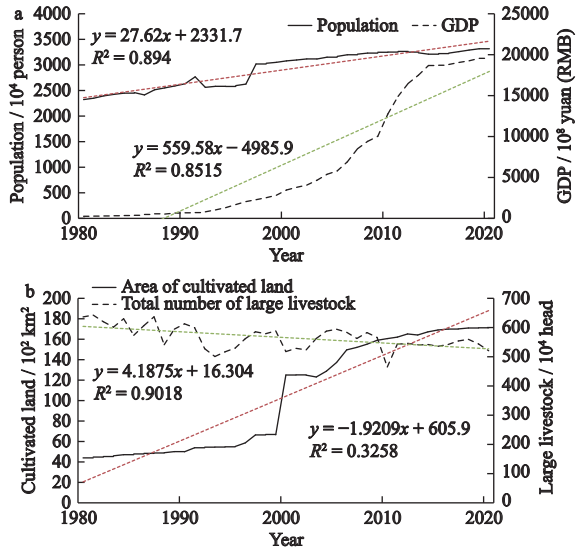

Fig. 6 Yearly change in social and economic data of the study area (a. population and GDP; b. area of cultivated land and total number of large livestock)

during past 40 yr. However, the number of large livestock at the end of the year showed a downward trend, from 6.36 million heads in 1980 to 5.21 million heads in 2020, accounting for a change of –18.08% (Fig. 6b).

3.2.3 Quantitative analysis of meteorological and socio-economic factors

To further clarify the influencing factors of dynamic changes in various types of landscapes and analyze the role and effectiveness of meteorological and socio-economic factors in the change process, the factors were quantitatively analyzed using principal components analysis (PCA). In the process of PCA, all kinds of parameters are annual data from 1980 to 2020, that is, the total number of each parameter is 40. The results show that the first principal component with a contribution rate of 59.64% was strongly correlated with the cultivated land area, GDP and total population, all of which had contribution rates of more than 90.00%. The second principal component with a contribution rate of 26.84% was strongly correlated to annual precipitation and annual average temperature, and was negatively correlated with the annual average temperature (Table 1). From a statistical point of view, the contribution rate of the first principal component is much higher than that of the second principal component, and socio-economic factors strongly affect dynamic changes in the lake landscape of SSL. Regional landscape evolution is a complex process of interaction between meteorological and socio-economic factors. Therefore, the next step will be to carry out the quantitative separation of meteorological and socio-economic factors in order to better determine the contribution rate of each factor.

Table 1 PCA (Principal Components Analysis) loading matrix of Songnen Sandy Land

Factors	PC1	PC2
Annual average wind speed	–0.945	0.076
Annual precipitation	0.037	0.807
Annual average temperature	0.158	–0.818
Total population	0.911	–0.217
GDP	0.921	0.192
Arable land area	0.949	–0.066
Number of large livestock at the end of the year	–0.630	0.104
Feature value	3.936	1.885
Contribution rate	59.636	26.838
Cumulative contribution rate	59.636	86.474

3.2.4 Relationship between driving factors and changes of sandy land-lake-vegetation landscape

The area of sandy land was positively correlated with the total population, area of cultivated land, and GDP, and negatively correlated with the annual average wind speed and the total number of large livestock at the end of the year (Table 2). The lake area was positively correlated with the annual average temperature and total population, and slightly negatively correlated with the annual average wind speed and annual precipitation. The areas of vegetation cover were positively correlated with the total number of large livestock, annual average wind speed, and annual precipitation at the end of the year, and negatively correlated with cultivated land area, GDP, and total population. This shows that changes in the sandy land-lake-vegetation landscape in SSL are closely related to climate change and human activities. Fluctuations in the annual precipitation decreased and that in the average annual average temperature increased. Overall, the trend of climate warming and drying is evident. This is consistent with the results of climate change research in Northeast China, such as those reported by He et al. (2013) and Sun et al. (2005). The increase in annual average temperature, slight decrease in annual precipitation can lead to the expansion of the sandy land area. In addition, the total population has increased from 1990, the demand for food has been increasing, and the cultivated area has also been continuously expanded. Various studies such as Guo et al. (2007) have also reported that population pressure is ex-

Table 2 Correlation analysis between sandy land area, vegetation area, lake area and climate factors and human factors

Landscape type	Annual precipitation	Annual average temperature	Annual average wind speed	Total population	Arable land area	Number of large livestock at the end of the year	GDP
Sandy land	–0.41	0.39	–0.86	0.94*	0.83	–0.86	0.61
Lake	–0.23	0.77	–0.42	0.56	0.34	0.38	0.04
Vegetation	0.55	0.39	0.86	–0.85	–0.96**	0.94*	–0.88*

Notes: * stands for significance < 0.05, ** stands for significance < 0.01

tremely high, and the excessive reclamation of land affects the development rate of area expansion in sandy lands.

4 Discussion

4.1 Mutual feedback relationship

The evolution of sandy land and changes in vegetation coverage are important surface processes in semi-arid areas (Zhang et al., 2011), and there are certain competition and dynamic equilibrium between sandstorm activities and vegetation cover (Li et al., 2009; El-Sheikh et al., 2010). The areas of vegetation cover in SSL during past 40 yr fluctuated and decreased, whereas the area of sandy land fluctuated and increased, which is consistent with the results of Wang et al. (2011). Studies on sand dunes and vegetation in the Kubuqi Desert and other areas have shown that vegetation affects the sand transportation capacity and transport direction of sediments by controlling the intensity and direction of near-surface airflow, which in turn affects the characteristics of erosion patterns and ultimately changes the spatial position and shape of dunes. When vegetation cover decreases, sand transportation and sand surface wind speed increase gradually. As a result, surface erosion is aggravated, and the rate of wind-sand activities is enhanced (Alamusa et al., 2017). Wind tunnel experiments also show that vegetation coverage can affect the grain size, structure, and wind erosion of near-surface wind-sand flow (Li et al., 2007). On the one hand, plant roots have a certain consolidation effect on the sand surface by retaining intercepted sand particles and promoting the growth and development of plants in sand dunes, and controlling the shape and development of sand dunes. On the other hand, wind-sand flow also changes the spatial distribution and community succession of dune vegetation through wind erosion or accumulation (Telfer et al., 2017). Lakes in sandy lands are an important part of the desert ecosystem and play an important role in maintaining ecological stability. Water is the first leading factor restricting the growth and survival of plants. Water has an important impact on the structure of the regional sand and air flow field and the transport of sand, thus determining the evolution process of the sandy land landscape in a certain buffer zone around the lake group (Dong et al., 2016). The competition and balance between oasisization and desertification reflected by changes in vegetation cover depends on the distribution of water resources and the coordination of the ecological environment, which affects the recharge of desert groundwater. Thus, the maintenance of the fragile wetland ecology in sandy lands depends on lakes (Du et al., 2018b).

4.2 Driving mechanism

SSL exhibited a clear trend of warm drying during past 40 yr. Over time, temperature increased, precipitation decreased, and potential evaporation increased. On the decadal scale, the lake area of SSL showed an upward fluctuation, which was significantly correlated with meteorological factors, such as annual average temperature, annual precipitation, and annual average wind speed. Changes in the landscape patterns of sandy lands and lakes are also the regional response of SSL to climate change (Jepsen et al., 2013). This has been confirmed by Schultz and Halpert (1995) through their research on the relationship between the global vegetation index and precipitation and temperature changes. Tucker et al. (1991) found that the expansion and shrinkage of the marginal vegetation in the Sahara Desert had a high degree of consistency with the variability of rainfall, accompanied by the expansion and contraction of sand dunes.

On an interannual scale, short-term high-intensity human activities can accelerate or delay the evolution of sand and lake landscapes. Davies et al. (2006) analyzed the relationship between human resources indicators, comprising GDP, population density, urban and rural

land usage, and NDVI from a global perspective. Their findings revealed the role and contribution of human activities in global ecological environment change. Gui et al. (2010) further pointed out that lake changes in the Songnen Plain in Northeast China are jointly affected by human activities and climate change, and large-scale climate change and human activities have exacerbated the trend of lake change. In SSL with the growth of population from 1980, the demand for food has increased, resulting in the expansion of sandy land and the sharp decline of lake area in the 1990s. After the 2000s, China promulgated and implemented the policy of conversion of farmland to wetland. In particular, the implementation of the river and lake system connection project in 2011, as well as policies to expand lake humidification, conversion of farmland to wetland, ecological wetland protection, *etc*., have effectively slowed down the reduction of lake area. Existing research on the driving forces of sandy land extension mainly considers natural factors as well as human factors, such as population and economic factors. However, the influence of institutional factors remains poorly understood, leading to insufficient explanations of the causes and formation mechanism of desertification. Institutional factors include ownership issues, conventional policies, and policy failure. Their effect on desertification is an important topic in the study of the genetic mechanisms of desertification. The next step is to analyze the mechanism of institutional factors and express them quantitatively.

5 Conclusions

The sandy land-lake-vegetation landscape of SSL exhibits its dynamic evolutionary characteristics. The overall growth rate of the area of sandy land in SSL during past 40 yr was 0.38%/yr. In particular, between 2000 and 2020, the area of sandy land showed a continuous decline. The overall area of lakes also increased by 29.73%, after which it expanded and then shrunk. The area of lakes increased by 0.80%/yr during 1980–2000, but it decreased at a rate of 3.30%/yr during 2000–2020. Overall, vegetation cover showed a decreasing trend, with high vegetation cover and low vegetation cover changing at rates of 0.17%/yr and –0.67%/yr, respectively, and the area of medium vegetation cover increased at 1.12%/yr. The sandy land, lakes, and vegetation in SSL showed significant interactions between them, with the areas of sandy land and vegetation cover, especially low vegetation cover, showing strong correlations.

The dynamic variations of the sandy land-lake-vegetation landscape in SSL are sensitive to climate change and human activities. During the last 40 yr, annual precipitation exhibited a downward fluctuation, annual average temperature exhibited an upward fluctuation and the trend of climate warming and drying was distinct. Consequently, the area of potential sandy land increased to a certain extent. In addition, the increase in regional total population increased the demand for food. With activities such as land reclamation around lakes and expansion of cultivated land, short-term high-intensity human activities can accelerate or delay the evolution rate of sandy land, lakes, and vegetation surface landscapes.

In order to prevent the reduction of wetlands and coordinate the relationship between human activities and the natural environment in SSL, it is urgent to protect and rationally use lake water resources, and coordinate the relationship between industrial production, agricultural irrigation and lake water resources. Moreover, regional desertification control projects and river and lake connection projects, and effective inter-provincial water resources management measures are required to achieve regional sustainable development.

References

Abd El-Wahab R H, Al-Rashed A R, Al-Dousari A, 2018. Influences of physiographic factors, vegetation patterns and human-impacts on aeolian landforms in arid environment. *Arid Ecosystems*, 8(2): 97–110. doi: 10.1134/S2079096118020026

Ackerly D D, Cornwell W K, Weiss S B et al., 2015. A geographic mosaic of climate change impacts on terrestrial vegetation: which areas are most at risk. *PLoS One*, 10(6): e0130629. doi: 10.1371/journal.pone.0130629

Alamusa, Yang T T, Cao J et al., 2017. Soil moisture influences vegetation distribution patterns in sand dunes of the Horqin Sandy Land, Northeast China. *Ecological Engineering*, 105: 95–101. doi: 10.1016/j.ecoleng.2017.04.035

Al-Masrahy M A, Mountney N P, 2015. A classification scheme for fluvial-aeolian system interaction in desert-margin settings. *Aeolian Research*, 17: 67–88. doi: 10.1016/j.aeolia.2015.01.010

Amuti T, Luo G, 2014. Analysis of land cover change and its driving forces in a desert oasis landscape of southern Xinjiang, China. *Solid Earth Discussions*, 6(2): 1907–1947. doi: 10.5194/

sed-6-1907-2014

An L S, Liao K H, Zhu L et al., 2021. Influence of river-lake isolation on the water level variations of Caizi Lake, lower reach of the Yangtze River. *Journal of Geographical Sciences*, 31(4): 551–564. doi: 10.1007/s11442-021-1858-4

Bishop-Taylor R, Tulbure M G, Broich M, 2018. Impact of hydroclimatic variability on regional-scale landscape connectivity across a dynamic dryland region. *Ecological Indicators*, 94: 142–150. doi: 10.1016/j.ecolind.2017.07.029

Boulanger Y, Taylor A R, Price D T et al., 2017. Climate change impacts on forest landscapes along the Canadian southern boreal forest transition zone. *Landscape Ecology*, 32(7): 1415–1431. doi: 10.1007/s10980-016-0421-7

Carlson T N, Ripley D A, 1997. On the relation between NDVI, fractional vegetation cover, and leaf area index. *Remote Sensing of Environment*, 62(3): 241–252. doi: 10.1016/S0034-4257(97)00104-1

Chen H, Ju P J, Zhang J et al., 2020. Attribution analyses of changes in alpine grasslands on the Qinghai-Tibetan Plateau. *Chinese Science Bulletin*, 65(22): 2406–2418. doi: 10.1360/TB-2019-0619

Chen W, Li A J, Hu Y G et al., 2021. Exploring the long-term vegetation dynamics of different ecological zones in the farming-pastoral ecotone in northern China. *Environmental Science and Pollution Research*, 28(22): 27914–27932. doi: 10.1007/S11356-021-12625-2

Davies R G, Orme C D L, Olson V et al., 2006. Human impacts and the global distribution of extinction risk. *Proceedings of the Royal Society B:Biological Sciences*, 273(1598): 2127–2133. doi: 10.1098/rspb.2006.3551

Dong C Y, Wang N A, Chen J S et al., 2016. New observational and experimental evidence for the recharge mechanism of the lake group in the Alxa Desert, north-central China. *Journal of Arid Environments*, 124: 48–61. doi: 10.1016/j.jaridenv.2015.07.008

Dong Zhibao, Chen Weinan, Dong Guangrong et al., 1996. Influences of vegetation cover on the wind erosion of sandy soil. *Acta Scientiae Circumstantiae*, 16(4): 437–443. (in Chinese)

Du Huishi, Hasi E, Li Shuang et al., 2018a. Landscape evolution and influence factors of aeolian sand and lakes in Horqin sandy land. *Scientia Geographica Sinica*, 38(12): 2109–2117. (in Chinese)

Du Huishi, Wang Liangyu, Chen Zhiwen et al. , 2018b. Distribution of lakes in Songnen Sandy land for 5 periods since 1980 and their changes. Wetland Science, 16(3): 352 –356. (in Chinese)

El-Sheikh M A, Abbadi G A, Bianco P M, 2010. Vegetation ecology of phytogenic hillocks (nabkhas) in coastal habitats of Jal Az-Zor National Park, Kuwait: role of patches and edaphic factors. *Flora - Morphology, Distribution, Functional Ecology of Plants*, 205(12): 832–840. doi: 10.1016/j.flora.2010.01.002

Gui Zhifan, Xue Bin, Yao Shuchun et al., 2010. Responses of lakes in the Songnen Plain to climate change. *Journal of Lake Sciences*, 22(6): 852–861. (in Chinese)

Guo Jian, Wang Tao, Xue Xian et al., 2007. The status and causes of desertification in Songnen Sandy Land. *Journal of Arid Land Resources and Environment*, 21(5): 99–103. (in Chinese)

Gutman G, Ignatov A, 1998. The derivation of the green vegetation fraction from NOAA/AVHRR data for use in numerical weather prediction models. *International Journal of Remote Sensing*, 19(8): 1533–1543. doi: 10.1080/014311698215333

He Wei, Bu Rencang, Xiong Zaiping et al., 2013. Characteristics of temperature and precipitation in Northeastern China from 1961 to 2005. *Acta Ecologica Sinica*, 33(2): 519–531. (in Chinese)

Hengeveld G M, Schüll E, Trubins R et al., 2017. Forest Landscape Development Scenarios (FOLDS): A framework for integrating forest models, owners' behaviour and socio-economic developments. *Forest Policy and Economics*, 85: 245–255. doi: 10.1016/j.forpol.2017.03.007

Hesp P A, Smyth T A G, 2017. Nebkha flow dynamics and shadow dune formation. *Geomorphology*, 282: 27–38. doi: 10.1016/j.geomorph.2016.12.026

Heywood H, 1941. The physics of blown sand and desert dunes. *Nature*, 148(3756): 480–481. doi: 10.1038/148480a0

Hu G Y, Dong Z B, Zhang Z C et al., 2021. Wind regime and aeolian landforms on the eastern shore of Qinghai Lake, Northeastern Tibetan Plateau, China. *Journal of Arid Environments*, 188: 104451. doi: 10.1016/j.jaridenv.2021.104451

Hulme M, Kelly M, 1993. Exploring the links between desertification and climate change. *Environment:Science and Policy for Sustainable Development*, 35(6): 4–45. doi: 10.1080/00139157.1993.9929106

Jepsen S M, Voss C I, Walvoord M A et al., 2013. Sensitivity analysis of lake mass balance in discontinuous permafrost: the example of disappearing Twelvemile Lake, Yukon Flats, Alaska (USA). *Hydrogeology Journal*, 21(1): 185–200. doi: 10.1007/s10040-012-0896-5

Khatancharoen C, Tsuyuki S, Bryanin S V et al., 2021. Long-time interval Satellite image analysis on forest-cover changes and disturbances around protected area, Zeya State Nature Reserve, in the Russian Far East. *Remote Sensing*, 13(7): 1285. doi: 10.3390/rs13071285

Lancaster N, Baas A, 1998. Influence of vegetation cover on sand transport by wind: field studies at Owens Lake, California. *Earth Surface Processes and Landforms*, 23(1): 69–82. doi: 10.1002/(SICI)1096-9837(199801)23:1<69::AID-ESP823>3.0.CO;2-G

Li S, Liu X W, Li H C et al., 2007. A wind tunnel simulation of the dynamic processes involved in sand dune formation on the western coast of Hainan Island. *Journal of Geographical Sciences*, 17(4): 453–468. doi: 10.1007/s11442-007-0453-7

Li Zhenshan, Wang Yi, He Limin, 2009. Vegetation-erosion process in semiarid region: Ⅰ. Dynamical models. *Journal of Desert Research*, 29(1): 23–30. (in Chinese)

Ma X Y, Wang X C, Wang D H et al., 2016. Function of a landscape lake in the reduction of biotoxicity related to trace organic chemicals from reclaimed water. *Journal of Hazardous Ma-*

terials, 318: 663–670. doi: 10.1016/j.jhazmat.2016.07.050

Mayaud J R, Wiggs G F S, Bailey R M, 2017. A field-based parameterization of wind flow recovery in the lee of dryland plants. *Earth Surface Processes and Landforms*, 42(2): 378–386. doi: 10.1002/esp.4082

Qiu G Y, Li C, Yan C H, 2015. Characteristics of soil evaporation, plant transpiration and water budget of Nitraria dune in the arid Northwest China. *Agricultural and Forest Meteorology*, 203: 107–117. doi: 10.1016/j.agrformet.2015.01.006

Schultz P A, Halpert M S, 1995. Global analysis of the relationships among a vegetation index, precipitation and land surface temperature. *International Journal of Remote Sensing*, 16(15): 2755–2777. doi: 10.1080/01431169508954590

Smith I M, Fiorino G E, Grabas G P et al., 2021. Wetland vegetation response to record-high Lake Ontario water levels. *Journal of Great Lakes Research*, 47(1): 160–167. doi: 10.1016/j.jglr.2020.10.013

Statistics Bureau of Inner Mongolia Autonomous Region, 2021. *Inner Mongolia Autonomous Region Statistical Yearbook* (2020). Beijing: China Statistical Press. (in Chinese)

Statistical Bureau of Jilin Province, 2021. *Jilin Province Statistical Yearbook* (2020). Beijing: China Statistical Press. (in Chinese)

Statistical Bureau of Liaoning Province, 2021. *Liaoning Province Statistical Yearbook* (2020). Beijing: China Statistical Press. (in Chinese)

Steinberg K A, Eichhorst K D, Rudgers J A, 2020. Riparian plant species differ in sensitivity to both the mean and variance in groundwater stores. *Journal of Plant Ecology*, 13(5): 621–632. doi: 10.1093/jpe/rtaa049

Sun Fenghua, Yang Suying, Chen Pengshi, 2005. Climatic warming-drying trend in Northeastern China during the last 44 years and its effects. *Chinese Journal of Ecology*, 24(7): 751–755,762. (in Chinese)

Telfer MW, Hesse P P, Perez-Fernandez M et al., 2017. Morphodynamics, boundary conditions and pattern evolution within a vegetated linear dunefield. *Geomorphology*, 290: 85–100. doi: 10.1016/j.geomorph.2017.03.024

Tucker C J, Dregne H E, Newcomb W W, 1991. Expansion and contraction of the sahara desert from 1980 to 1990. *Science*, 253(5017): 299–300. doi: 10.1126/science.253.5017.299

Wang Liangyu, Du Huishi, 2018. Dynamic evolution and simulation prediction of aeolian vegetation in Songnen Sandy Land in recent 35 years. *Research of Soil and Water Conservation*, 25(4): 380–385. (in Chinese)

Wang M Y, Lu N, Li Q L et al., 2020. Contribution of plant traits to the explanation of temporal variations in carbon and water fluxes in semiarid grassland patches. *Journal of Plant Ecology*, 13(6): 773–784. doi: 10.1093/jpe/rtaa058

Wang Tao, Song Xiang, Yan Changzhen et al., 2011. Remote sensing analysis on aeolian desertification trends in northern China during 1975–2010. *Journal of Desert Research*, 31(6): 1351–1356. (in Chinese)

Wang Wenxiang, Zuo Dongdong, Feng Guolin, 2014. Analysis of the drought vulnerability characteristics in Northeast China based on the theory of information distribution and diffusion. *Acta Physica Sinica*, 63(22): 229201. (in Chinese)

Yang W, Zhang S W, 2012. Monitoring desertification process in Songnen Sandy Land during the past 10 years. *Advanced Materials Research*, 518–523: 4740–4744. doi: 10.4028/www.scientific.net/AMR.518-523.4740

Yang Wenbin, Wang Tao, Feng Wei et al., 2017. The theory and progress of sand control with low coverage. *Journal of Desert Research*, 37(1): 1–6. (in Chinese)

Yang Wenbin, Wang Tao, Xiong Wei et al., 2021. Overview of hydrological principle of low vegetation coverage sand control. *Journal of Desert Research*, 41(3): 75–80. (in Chinese)

Zhang M, Li G X, 2018. Combining TOPSIS and GRA for supplier selection problem with interval numbers. *Journal of Central South University*, 25(5): 1116–1128. doi: 10.1007/s11771-018-3811-y

Zhang Ping, Hasi Eerdun, Du Huishi et al. , 2011. Dynamic relationship between parabolic dunes and *Artemisia ordosica*. *Chinese Science Bulletin*, 56(35): 3003–3010. (in Chinese)

Zhao Y C, Gao X, Lei J Q et al., 2020. Nebkha alignments and their implications for shadow dune elongation under unimodal wind regime. *Geomorphology*, 365: 107250. doi: 10.1016/j.geomorph.2020.107250